

Non-isothermal crystallization kinetics of β -nucleated isotactic polypropylene

Yuan-Hong Shi · Qiang Dou

Received: 27 November 2011 / Accepted: 13 July 2012 / Published online: 26 August 2012
© Akadémiai Kiadó, Budapest, Hungary 2012

Abstract Isotactic polypropylenes (iPP) samples were incorporated with two β -nucleating agents (NT-A and NT-C), respectively, and their non-isothermal crystallization and subsequent melt behaviors were investigated by means of differential scanning calorimeter. Jeziorny, Ozawa, and Mo methods were used to analyze non-isothermal crystallization kinetics of pure iPP and β -nucleated iPP samples. The activation energies (ΔE) of non-isothermal crystallization were calculated by Kissinger method. And the nucleation activities were calculated according to the Dobreva method. It is found that the crystallization temperature decreases and the crystallization rate increases with increasing cooling rate. The crystallization temperature and crystallization rate of nucleated iPP are higher than those of pure iPP. The order of ΔE is NT-A/iPP > pure iPP > NT-C/iPP. NT-C is more efficient than NT-A as a β -nucleating agent. But the non-isothermal crystallization kinetics of α - and β -phases cannot be determined separately. The present results should be considered with caution.

Keywords Isotactic polypropylene · β -Nucleating agent · Non-isothermal crystallization kinetics · Activation energy · Nucleation activity

Introduction

Isotactic polypropylene (iPP) is one of the most common thermoplastic, which is widely used in industry because it has good mechanical properties, feasible processing, and low

price. It is well known that iPP is a polymorphic polymer, which can develop α , β , γ , δ , and smectic phases under different conditions. β -iPP has higher impact strength and excellent ductility than α -iPP, thus it attracts many researchers' attention. β -iPP can be obtained by some methods such as isothermal crystallization under a certain temperature [1], temperature gradient [2], shear [3], and the addition of β -nucleating agent. Among them, the addition of β -nucleating agent is the most efficient way to obtain high pure β -iPP. There are mainly four classifications of β -nucleating agents. The first one is organic pigment such as γ -quinacridone [4, 5] and quinacridonequinone [6]. The second one is amide, such as N,N' -dicyclohexyl-2,6-naphthalenedicarboxamide [7], N,N' -diphenyl glutaramide [8], N,N' -diphenyl adipamide [9], and N,N' -dicyclohexylsuccinamide [10]. Recently, Varga et al. [11] found tris-2,3-dimethyl-hexylamide of trimesic acid was an active β -nucleating agent and possessed dual nucleating ability. The third one is some metallic salts of dicarboxylic acids or their mixtures, such as a mixture of pimelic acid and calcium stearate [12], calcium pimelate and calcium suberate [13, 14], and metallic salts of pimelic acid, malonic acid, and glutaric acid [15–17]. The fourth one is some rare earth compounds such as compounds of lanthanum [18, 19]. Addition of β -nucleating agent not only increases the content of β crystal but also makes the size of spherulite small.

Mechanical and physical properties of crystalline polymer are decided by crystal structure and morphology, which in turn is influenced by crystallization behavior of polymer. Thus, study of isothermal and non-isothermal crystallization kinetics is very important to understand the properties of polymeric products. Because practical processing undergoes non-isothermal crystallization progress, study of non-isothermal kinetics has practical significance. Many models, such as Jeziorny model [20–23], Ozawa

Y.-H. Shi · Q. Dou (✉)
College of Materials Science and Engineering,
Nanjing University of Technology, Nanjing 210009, China
e-mail: douqiang.njut@163.com

model [24, 25], Mo model [20–23, 26–30], and so on [31–33], were used to describe non-isothermal crystallization kinetics of nucleated PP and PP composites. Ahangari et al. [25] reported that Ozawa method was fit for pristine iPP but not for iPP/SWCNTs nanocomposite, while Caze-Chuah and Ziabicki models were successfully used to describe the non-isothermal crystallization processes of iPP and its nanocomposite. Supaphol et al. [33] reported that Avrami, Urbanovici–Segal, Ozawa, and Ziabicki models well described non-isothermal melt-crystallization kinetics of sPP resins having different molecular characteristics. Zhang et al. [34] suggested that both the modified Avrami theory of Jeziorny and Mo method were fit for non-isothermal crystallization kinetics of iPP nucleated with 1,3:2,4-bis(3,4-dimethylbenzylidene) sorbitol.

In this work, differential scanning calorimeter (DSC) was used to investigate non-isothermal crystallization and subsequent melting behavior of iPPs nucleated by two kinds of commercial β -nucleating agents (NT-A and NT-C), respectively. The non-isothermal crystallization kinetics of pure iPP and nucleated iPP were analyzed by different models, namely Jeziorny, Ozawa, and Mo models. The activation energies for non-isothermal crystallization (ΔE) of pure iPP and nucleated iPP were calculated by the method of Kissinger. Furthermore, the nucleation activity was calculated by the method proposed by Dobreva and Gutzow.

Experimental

Materials

iPP pellets (Grade F401, MFR = 1.2 dg min⁻¹ under 230 °C and 21.2 N, Sinopec Yangzi Petrochemical Co., Ltd., Nanjing, China), β -nucleating agents (NT-A and NT-C, carboxylates, FTIR spectra are shown in Fig. 1, Nanjing Chengkuan Trade Co., Ltd., Nanjing, China), and liquid paraffin (Shanghai Lingfeng Chemical Reagent Co., Ltd., Shanghai, China) were used in this work.

Preparation of samples

iPP pellets were premixed with 0.05 mass% liquid paraffin and 0.1 mass% β -nucleating agent. The mixtures were compounded in a twin-screw extruder (TE-20, $D = 20$ mm, $L/D = 32/1$, Coperion Keya Machinery Co., Ltd., Nanjing, China). The melt temperature was 205 °C, and the main screw speed was 200 rpm. The melt was cooled and pelletized. Nucleated iPP pellets were used in DSC analysis. The blank iPP sample without β -nucleating agent was also prepared in a similar way.

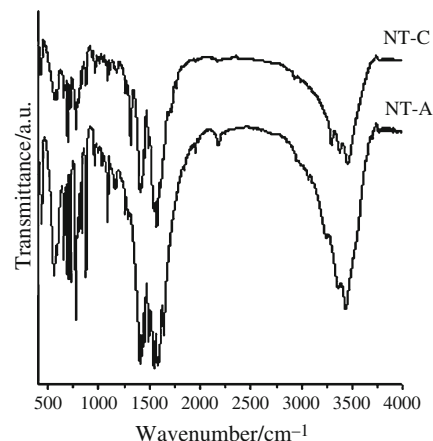


Fig. 1 FTIR spectra of NT-A and NT-C

DSC analysis

Non-isothermal crystallization exotherms and subsequent melting endotherms were recorded with a ZF-DSC-D2 DSC instrument (Shanghai Zufa Industry Co., Ltd., Shanghai, China) in a dry nitrogen atmosphere. The temperature and heat flow were calibrated with indium, stannum, and zinc. Each sample of 5–6 mg was heated from room temperature to 210 °C at 10 °C min⁻¹ and held at 210 °C for 5 min to remove thermal history. After that, the sample was cooled to 50 °C at 20, 15, 10, and 5 °C min⁻¹, respectively. Subsequent melting behavior was studied by reheating the sample to 210 °C at 10 °C min⁻¹.

In order to characterize the β -form content of the sample exactly, the disturbing effect of the β to α recrystallization should be eliminated. This recrystallization occurs during partial melting of the β -phase in the samples which were cooled below the critical temperature ($T_R^* = 100$ – 105 °C), as pointed out by Varga et al. [7, 35]. Additional experiments were performed. The melted samples were cooled to 100 °C, and held for 5 min. Finally, the samples were reheated to 210 °C. Both the heating and cooling rates were 10 °C min⁻¹. The peak melting temperatures of α phase ($T_{m,\alpha}$) and β phase ($T_{m,\beta}$) were recorded. The contents of β -crystalline form (K_{DSC}) were calculated as Eq. (1):

$$K_{DSC} = [A_\beta / (A_\alpha + A_\beta)] \times 100 \% \quad (1)$$

where A_α and A_β are the areas of α and β melting peaks, respectively.

Results and discussion

Non-isothermal crystallization behavior

Non-isothermal crystallization exotherms are shown in Fig. 2, and the peak temperatures of crystallization (T_c^p) are

Fig. 2 Non-isothermal crystallization exotherms: **a** pure iPP, **b** 0.1 % NT-A/iPP, and **c** 0.1 % NT-C/iPP

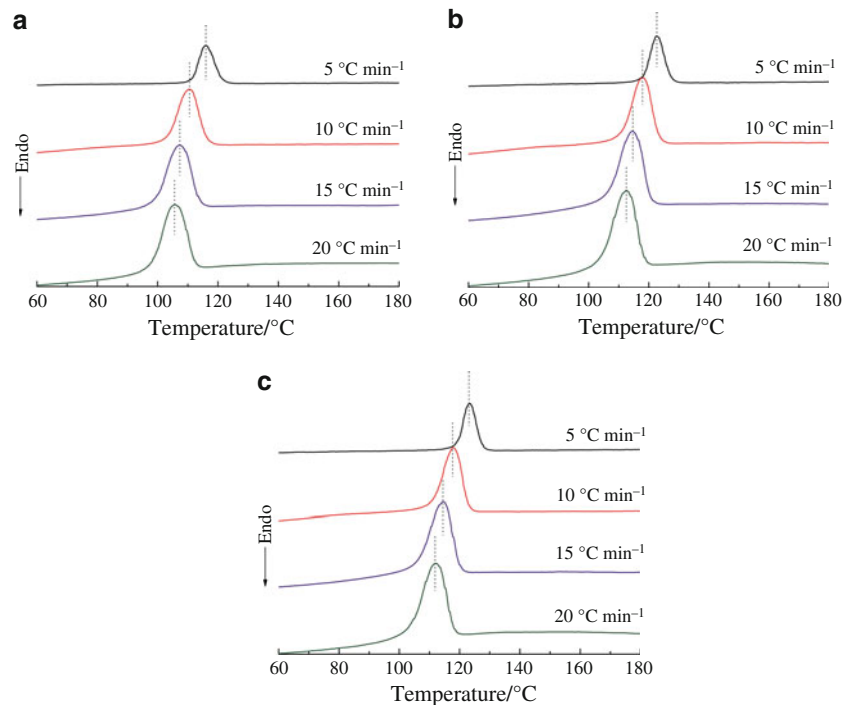


Table 1 T_c^p and $t_{1/2}$ of pure iPP and nucleated iPP

Cooling rate, $\Phi/^\circ\text{C min}^{-1}$	Pure iPP		0.1 %NT-A/iPP		0.1 %NT-C/iPP	
	$T_c^p/^\circ\text{C}$	$t_{1/2}/\text{min}$	$T_c^p/^\circ\text{C}$	$t_{1/2}/\text{min}$	$T_c^p/^\circ\text{C}$	$t_{1/2}/\text{min}$
5	116.0	2.12	122.7	2.08	123.4	1.66
10	110.5	1.27	118.1	1.10	118.0	0.93
15	107.3	0.79	114.5	0.75	114.6	0.69
20	105.7	0.61	112.5	0.60	112.1	0.52

listed in Table 1. For all samples, exothermic trace becomes wider and shifts to low temperature and T_c^p decreases with increasing cooling rate used. When the cooling rate increases from 5 to 20 $^\circ\text{C min}^{-1}$, T_c^p of pure iPP, 0.1 % NT-A/iPP and 0.1 % NT-C/iPP decreases from 116, 122.7, and 123.4 $^\circ\text{C}$ to 105.7, 112.5, and 112.1 $^\circ\text{C}$, respectively. At a lower cooling rate, polymer chain has enough time to transfer from the melt to the surface of the crystal, so crystallization can occur at higher temperature. At the same cooling rate, T_c^p of nucleated iPP is higher than that of pure iPP, for instance, at 10 $^\circ\text{C min}^{-1}$, T_c^p of pure iPP, 0.1 % NT-A/iPP and 0.1 % NT-C/iPP is 110.5, 118.1, and 118.0 $^\circ\text{C}$, respectively. Addition of nucleating agent introduces a large number of active sites into iPP melt, making nucleation density increase, so crystallization can occur at higher temperature.

In DSC, the heat release during the non-isothermal melt-crystallization process seems to be a function of temperature rather than time, as in the case of isothermal

crystallization process. Therefore, the relative crystallinity $X(T)$ as a function of temperature can be expressed as follows:

$$X(T) = \frac{\int_{T_0}^T (dH_c/dT)dT}{\int_{T_0}^{T_\infty} (dH_c/dT)dT} \quad (2)$$

Here, T_0 , T , and T_∞ are the initial, arbitrary, and final crystallization temperatures, respectively. dH_c is the fusion of the heat release in infinitesimal temperature interval dT .

$X(T)$ as a function of temperature of pure and nucleated iPP is shown in Fig. 3. All curves show reverse S-curves. According to the relationship between time (t) and temperature (T), $t = (T_0 - T)/\Phi$ (Φ , the cooling rate), abscissa of temperature can transform to timescale, and relative crystallinity $X(t)$ as a function of time of pure and nucleated iPP is shown in Fig. 4. All curves exhibit typical S-curves. Crystallization time with 50 % relative crystallinity ($t_{1/2}$) can be obtained from Fig. 4 and is listed in Table 1. For all samples, $t_{1/2}$ decreases with increasing cooling rate used, indicating that crystallization rate increases with increasing cooling rate. When the cooling rate increases from 5 to 20 $^\circ\text{C min}^{-1}$, $t_{1/2}$ of pure iPP, 0.1 % NT-A/iPP, and 0.1 % NT-C/iPP decreases from 2.12, 2.08, and 1.66 min to 0.61, 0.60, and 0.52 min, respectively. At the same cooling rate, $t_{1/2}$ is in the order of pure iPP > 0.1 % NT-A/iPP > 0.1 % NT-C/iPP, which suggests that the addition of nucleating agent makes crystallization rate increase. Furthermore, the crystallization rate of NT-C/iPP is higher than that of NT-A/iPP.

Fig. 3 Relative crystallinity $X(T)$ as a function of temperature observed at different cooling rate: **a** pure iPP, **b** 0.1 % NT-A/iPP, and **c** 0.1 % NT-C/iPP

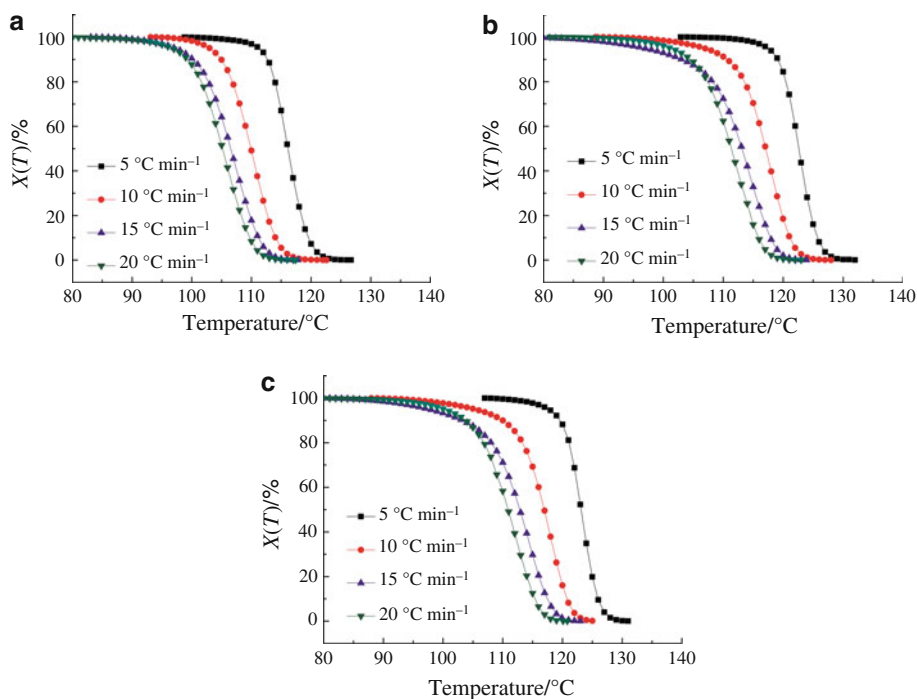
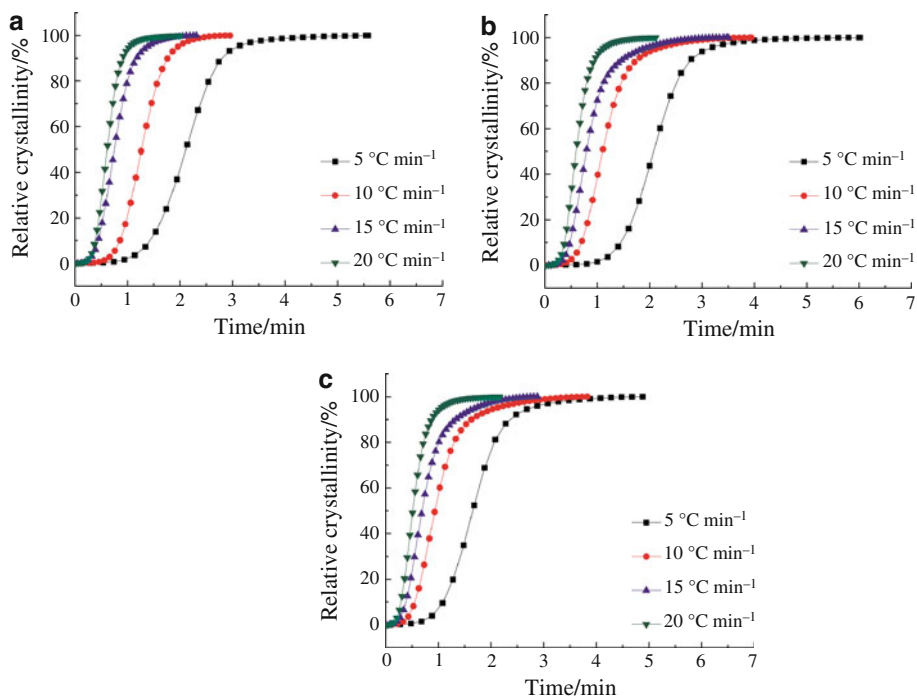


Fig. 4 Relative crystallinity $X(t)$ as a function of time observed at different cooling rate: **a** pure iPP, **b** 0.1 % NT-A/iPP, and **c** 0.1 % NT-C/iPP



Non-isothermal crystallization kinetics

Jeziorny model

Avrami [36–38] first proposed an equation for describing isothermal crystallization kinetics, which can be described as:

$$1 - X(t) = \exp(-Zt^n) \tag{3}$$

Taking a double logarithm of Eq. (3) gives:

$$\lg[-\ln(1 - X(t))] = \lg Z + n \lg t \tag{4}$$

where $X(t)$ is the relative crystallinity at arbitrary time t , Z is the crystallization rate constant, and n is the Avrami

Fig. 5 $\lg[-\ln(1 - X(t))]$ as a function of $\lg t$ based on Eq. (4): **a** pure iPP, **b** 0.1 % NT-A/iPP, and **c** 0.1 % NT-C/iPP

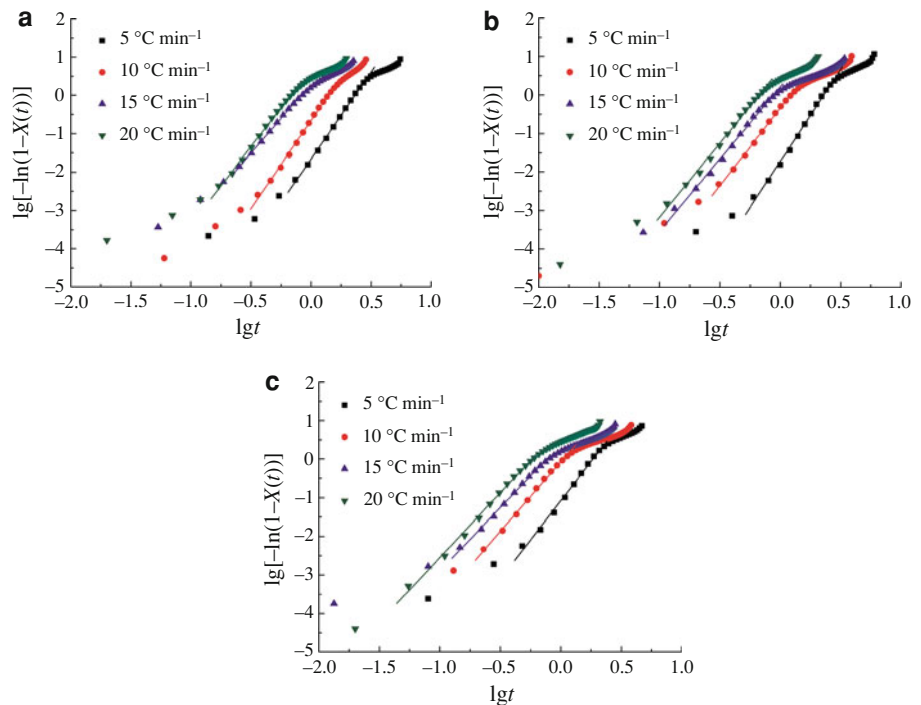


Table 2 Z_c , n , and r^2 obtained from Fig. 5

Sample	$\Phi/^\circ\text{C min}^{-1}$	Z_c	n	The average value of n	r^2
Pure iPP	5	0.45	4.54	4.21	0.9985
	10	0.86	4.59		0.9973
	15	1.05	3.63		0.9993
	20	1.08	4.08		0.9972
0.1 % NT-A/iPP	5	0.45	4.78	4.11	0.9960
	10	0.93	4.05		0.9970
	15	1.03	3.76		0.9977
	20	1.08	3.85		0.9947
0.1 % NT-C/iPP	5	0.61	4.04	3.56	0.9943
	10	0.98	3.60		0.9978
	15	1.06	3.28		0.9974
	20	1.10	3.35		0.9950

exponent, which relates to nucleation mechanism and the geometry of crystal growth. $\lg Z$ and n are intercept and slope of the plot of $\lg[-\ln(1 - X(t))]$ versus $\lg t$, respectively.

Jeziorny [39] modified Z with the cooling rate Φ to analyze non-isothermal crystallization process:

$$\lg Z_c = \lg Z / \Phi \tag{5}$$

Figure 5 shows the plots of $\lg[-\ln(1 - X(t))]$ versus $\lg t$ of pure iPP and nucleated iPP, and Z_c , n , and r^2 (a measure of goodness-of-fit of linear regression) are listed in Table 2.

According to the value of r^2 , the linear dependences of the central parts of the curves present were found. In the research of Zeng et al. [19], the deviation after linear part was probably due to the secondary crystallization, and some initial dots were not considered because logarithmic plotting tended to overestimate small errors in the assessment of the initial time of crystallization. For all samples, Z_c increases with the cooling rate, suggesting that crystallization rate increases with the cooling rate. When the cooling rate increases from 5 to 20 $^\circ\text{C min}^{-1}$, Z_c of pure iPP, 0.1 % NT-A/iPP, and 0.1 % NT-C/iPP increases from 0.45, 0.45, and 0.61 to 1.08, 1.08, and 1.10, respectively. At the same cooling rate, Z_c of nucleated iPP is higher than that of pure iPP, indicating that the addition of nucleating agents increase crystallization rates. When the cooling rate is 10 $^\circ\text{C min}^{-1}$, Z_c of pure iPP, 0.1 % NT-A/iPP, and 0.1 % NT-C/iPP are 0.86, 0.93, and 0.98, respectively. The average value of n decreases with addition of nucleating agent, indicating that nucleating agent changes the nucleation style and crystal growth manner of iPP.

Ozawa model

Considering the influence of the cooling rate, Ozawa [40] extended Avrami equation to describe non-isothermal crystallization process, and derived an equation for non-isothermal crystallization kinetics of polymer with constant cooling rate Φ :

$$1 - X(T) = \exp[-K(T)/\Phi^m] \tag{6}$$

The double logarithm expression of Eq. (6) gives:

$$\lg[-\ln(1 - X(T))] = \lg K(T) - m \lg \Phi \tag{7}$$

where $K(T)$ is a function of temperature, which relates to nucleation style, nucleation rate, and crystal growth rate.

Figure 6 is the plots of $\lg[-\ln(1 - X(T))]$ versus $\lg \Phi$ at different temperature of pure iPP and nucleated iPP based on Eq. (7). $\lg K(T)$ and m are obtained from the intercept and slope of the fitting line, which are listed in Table 3. For all samples, $\lg K(T)$ and m increase with increasing temperature. At the same temperature, $\lg K(T)$ and m are in the order of pure iPP > 0.1 % NT-C/iPP > 0.1 % NT-A/iPP. Obviously, the crystallization process of iPP is changed by the addition of β -nucleating agent. For pure iPP, in the plot of $\lg[-\ln(1 - X(T))]$ versus $\lg \Phi$, there are only three dots at 116 °C and two dots at 118 and 120 °C, respectively, because crystallization temperature is low at high cooling

rate (15 and 20 °C min⁻¹). According to r^2 in Table 3, for nucleated iPP, linear dependence is found at low temperature; while it does not exist at high temperature, especially for 0.1 % NT-C/iPP.

Tjong and Xu [24] reported that the non-isothermal crystallization of β -PP and its composites with CaCO₃ follows the Ozawa equation. Ahangari et al. [25] found that the secondary crystallization of iPP/SWCNTs nanocomposite should not be neglected and Ozawa model failed to describe the crystallization behavior of iPP/SWCNTs nanocomposite.

Mo model

Liu et al. [41] developed a new method for non-isothermal crystallization by combining Avrami and Ozawa models, as expressed in following:

Fig. 6 $\lg[-\ln(1 - X(T))]$ as a function of $\lg \Phi$ at different temperature based on Eq. (7): **a** pure iPP, **b** 0.1 % NT-A/iPP, and **c** 0.1 % NT-C/iPP

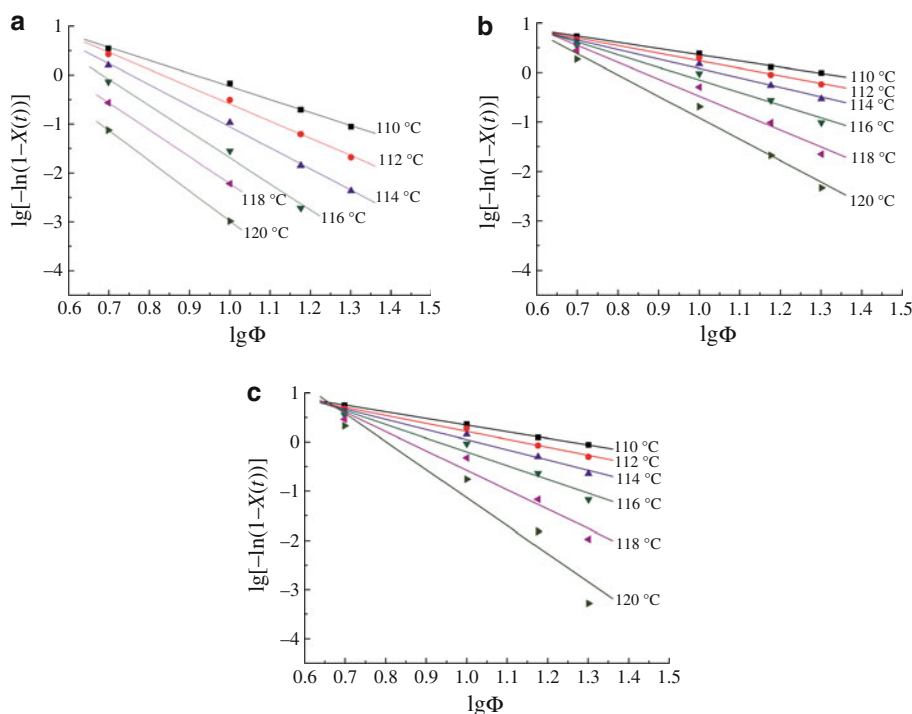
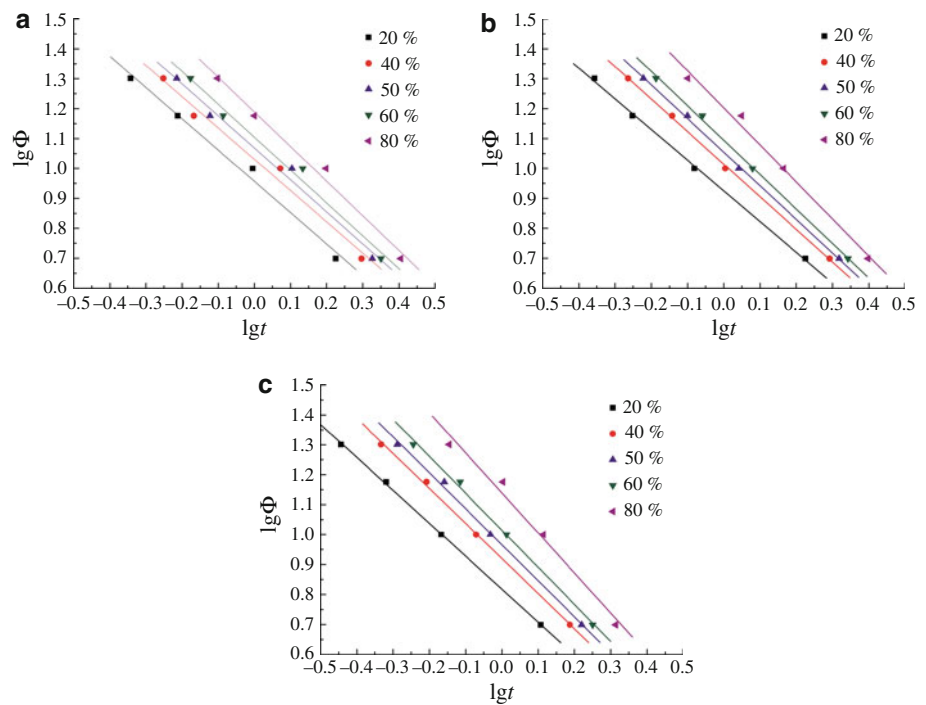


Table 3 $\lg K(T)$, m , and r^2 obtained from Fig. 6

Temperature/°C	Pure iPP			0.1 %NT-A/iPP			0.1 %NT-C/iPP		
	$\lg K(T)$	m	r^2	$\lg K(T)$	m	r^2	$\lg K(T)$	m	r^2
110	2.44	2.67	0.9965	1.62	1.26	0.9950	1.70	1.35	0.9988
112	2.92	3.51	0.9963	1.77	1.53	0.9893	1.84	1.62	0.9889
114	3.24	4.30	0.9973	1.99	1.91	0.9844	2.12	2.07	0.9775
116				2.40	2.55	0.9762	2.59	2.80	0.9666
118				2.94	3.42	0.9715	3.36	3.94	0.9581
120				3.40	4.32	0.9801	4.56	5.69	0.9303

Fig. 7 $\lg\Phi$ as a function of $\lg t$ at different relative crystallinity based on Eq. (8)



$$\lg\Phi = \lg F(T) - \alpha \lg t \tag{8}$$

$\lg\Phi$ is linear with $\lg t$, the intercept is $\lg F(T)$, and the slope is $-\alpha$. A high value of $F(T)$ means that a high cooling rate needs to reach a certain relative crystallinity in unit crystallization time, which reflects difficult extent of crystallization. $\alpha = n/m$, n is apparent Avrami exponent of non-isothermal crystallization, and m is Ozawa exponent.

Figure 7 shows the plot of $\lg\Phi$ versus $\lg t$ at different relative crystallinity of pure iPP and nucleated iPP based on Eq. (8), and $F(T)$, α and r^2 are listed in Table 4. $F(T)$ increases with increasing relative crystallinity, which suggests that the cooling rate should be increased to reach a higher relative crystallinity in unit crystallization time. When the relative crystallinity increases from 20 to 80 %, $F(T)$ of pure iPP, 0.1 % NT-A/iPP, and 0.1 % NT-C/iPP increases from 9.06, 8.41, and 6.57 to 15.45, 15.94, and 13.78, respectively. At the same relative crystallinity, $F(T)$ is in the order of pure iPP > 0.1 % NT-A/iPP > 0.1 % NT-C/iPP, which indicates that 0.1 % NT-C/iPP

needs lower cooling rate, that is to say, crystallization rate of 0.1 % NT-C/iPP is the fastest. When the relative crystallinity is 50 %, $F(T)$ of pure iPP, 0.1 % NT-A/iPP, and 0.1 % NT-C/iPP is 11.71, 11.34, and 9.25, respectively. α increases with increasing relative crystallinity, α is in the order of 0.1 % NT-C/iPP > 0.1 % NT-A/iPP > pure iPP. According to the value of r^2 shown in Table 4, significant linear correlations between $\lg\Phi$ and $\lg t$ are observed for all samples, indicating that Mo model describes the non-isothermal crystallization of pure iPP and nucleated iPP well. The results show that the crystallization rate is in the order of 0.1 % NT-C/iPP > 0.1 % NT-A/iPP > pure iPP, which is similar to Z_c and $t_{1/2}$.

Zhang et al. [20] found that Mo method could describe non-isothermal crystallization kinetics of iPP nucleated with a novel highly efficient supported β -nucleating agent (NT100, calcium pimelate supported on the surface of nano- CaCO_3) well, $F(T)$ of 5 % NT100/95 % iPP (1.8–3.3) was lower than that of pure iPP (3.4–6.4). Yang et al. [26,

Table 4 $F(T)$, α , and r^2 obtained from Fig. 7

Relative crystallinity/%	Pure iPP			0.1 % NT-A/iPP			0.1 % NT-C/iPP		
	$F(T)$	α	r^2	$F(T)$	α	r^2	$F(T)$	α	r^2
20	9.06	1.05	0.9894	8.41	1.03	0.9988	6.57	1.10	0.9996
40	10.73	1.05	0.9835	10.33	1.09	0.9993	8.32	1.17	0.9988
50	11.71	1.07	0.9863	11.34	1.12	0.9993	9.25	1.20	0.9975
60	12.72	1.10	0.9866	12.43	1.15	0.9986	10.33	1.24	0.9969
80	15.45	1.16	0.9885	15.94	1.23	0.9906	13.78	1.34	0.9836

27] reported that Mo method could satisfactorily describe the non-isothermal crystallization behavior of β -nucleated PP, β -nucleated PP/PA6, and β -nucleated PP/PA6/PP-g-MA blends; $F(T)$ increased with the relative crystallinity, and the value of α increased slightly. Zhang et al. [34] reported that Mo method was suitable for the non-isothermal crystallization kinetics of iPP nucleated with 1,3:2,4-bis(3,4-dimethylbenzylidene) sorbitol (DMDBS), as $F(T)$ of virgin iPP and iPP/DMDBS are 2.85–4.29 and 1.21–1.64, respectively. Wang and Dou [42] found that Ozawa model could not be applied to N,N',N'' -tris-tert-butyl-1,3,5-benzene-tricarboxamide/iPP system but Mo model could, and both α and $F(T)$ increased with the relative crystallinity.

Activation energy for non-isothermal crystallization

Taking the influence of different cooling rate on crystallization process into account, Kissinger [43] proposed an equation for calculating the activation energy (ΔE) during non-isothermal crystallization process:

$$d\left[\ln\left(\Phi/T_p^2\right)\right]/d(1/T_p) = -\Delta E/R \quad (9)$$

where Φ is the cooling rate, R is gas constant ($8.314 \text{ J K}^{-1} \text{ mol}^{-1}$), T_p is the peak crystallization temperature. Integral expression of Eq. (9) gives:

$$\ln\left(\Phi/T_p^2\right) = (1/T_p)(-\Delta E/R) \quad (10)$$

It is noted that ΔE defined by Kissinger is the activation energy that polymer chains need to migrate from melt to the surface of crystal. ΔE reflects difficult extent of crystal growth. ΔE can be obtained from the slope in the plot of $\ln\left(\Phi/T_p^2\right)$ versus $1/T_p$.

$\ln\left(\Phi/T_p^2\right)$ as a function of $1/T_p$ of pure iPP and nucleated iPP based on Eq. (10) is shown in Fig. 8 and the activation energy (ΔE) is calculated from Fig. 8. ΔE of pure iPP, 0.1 % NT-A/iPP, and 0.1 % NT-C/iPP are $167.18 \text{ kJ mol}^{-1}$, $195.92 \text{ kJ mol}^{-1}$, and $152.25 \text{ kJ mol}^{-1}$,

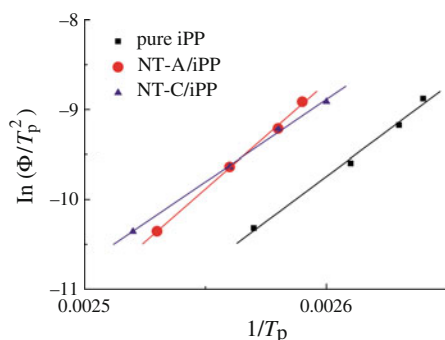


Fig. 8 $\ln\left(\Phi/T_p^2\right)$ as a function of $1/T_p$ based on Eq. (10)

respectively. That is to say, the addition of NT-A increases ΔE , while NT-C decreases ΔE .

From the viewpoint of the activation energy, the decrease of ΔE is favorable to increase the crystallization rate, which is confirmed by the fact that the addition of 0.1 % NT-C decreases ΔE and increases the crystallization rate. Zhang et al. [20] found that ΔE of β -iPP was lower than that of pure iPP and decreased with the increasing content of β -crystal.

While the addition of 0.1 % NT-A increases ΔE and the crystallization rate synchronously. Zhao et al. [31] found that the addition of cadmium bicycle [2.2.1] hept-5-ene-2,3-dicarboxylate could obviously shorten $t_{1/2}$, while slightly increasing ΔE of iPP. Wei et al. [44] also found that the addition of WBG slightly increased the ΔE of iPP. They believed that strong interaction between nucleating agents and segments of iPP might baffle the transfer of macromolecular segments from iPP melts to the crystal growth surface, resulting in the increase of ΔE ; while nucleation was the controlling step during crystallization, the increasing of nucleation rate led to the increase of the overall crystallization rate. The difference of ΔE between NT-A and NT-C nucleated iPP reflects the different nucleation and crystallization ability of the two nucleated iPP.

Nucleation activity

The nucleating activity φ refers to a factor by which the work of nucleation decreases by adding a foreign substance; if the foreign substrate is extremely active $\varphi = 0$, while for inert particles $\varphi = 1$. φ can be calculated from the following equation proposed by Dobreva and Gutzow [45, 46]:

$$\Phi = B_s^*/B_s \quad (11)$$

Here, B_s^* and B_s are experiential parameters for nucleated iPP and blank iPP, respectively. B_s^* and B_s can be determined from Eqs. (12) and (13) by plotting $\ln\Phi$ versus $1/\Delta T_p^2$ (ΔT_p , the undercooling):

$$\ln\Phi = C - B_s^*/\Delta T_p^2 \quad (12)$$

$$\ln\Phi = C - B_s/\Delta T_p^2 \quad (13)$$

The plots of $\ln\Phi$ versus $1/\Delta T_p^2$ for pure iPP and nucleated iPP are shown in Fig. 9, B_s^* and B_s can be obtained from the slope, and φ can be obtained according to Eq. (11). Because of the presence of double melting temperatures, B_s^* and B_s of α and β forms are obtained, respectively, and relevant φ is listed in Table 5. For all cases, $\varphi < 1$, and φ of NT-C is lower than that of NT-A, which shows that both NT-A and NT-C are effective β -nucleating agents, and NT-C is more effective than NT-A.

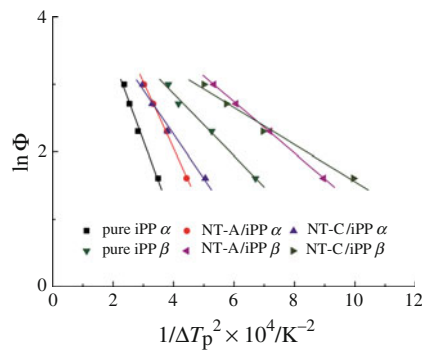


Fig. 9 $\ln\Phi$ as a function of $1/\Delta T_p^2$

Table 5 φ obtained from Fig. 9 and Eq. (11)

Nucleating agent	φ	
	α -Phase	β -Phase
NT-A	0.81	0.83
NT-C	0.54	0.60

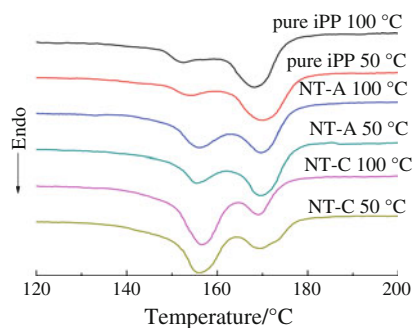


Fig. 10 Subsequent melting curves of pure and nucleated iPP after cooling to different end cooling temperatures. The heating and cooling rates are $10\text{ }^\circ\text{C min}^{-1}$

Comparison of melting behaviors with different end cooling temperatures

Subsequent melting endotherms of pure and nucleated iPP after cooling to different end cooling temperatures are shown in Fig. 10. In all melting curves, two peaks are observed at about 155 and 168 °C, which represent the melting peaks of β - and α -phases, respectively. For pure iPP, the melting peak of β -phase is small, and that of α -phase is large. With the addition of β -nucleating agent, the melting peak of β -phase becomes large and that of α -phase becomes small, especially for NT-C nucleated iPP.

$T_{m,\alpha}$, $T_{m,\beta}$, and K_{DSC} of pure iPP and nucleated iPP are listed in Table 6. K_{DSC} of the sample with the end cooling temperature of 50 °C is lower than that with the end cooling temperature of 100 °C. It reflects that β - α recrystallization occurs when the end cooling temperature is

Table 6 $T_{m,\alpha}$, $T_{m,\beta}$, and K_{DSC} of pure iPP and nucleated iPP

Sample	The end cooling temperature/ $^\circ\text{C}$	$T_{m,\alpha}/^\circ\text{C}$	$T_{m,\beta}/^\circ\text{C}$	$K_{DSC}/\%$
Pure iPP	100	168.3	152.7	20.8
	50	170.2	154.8	15.19
0.1 %NT-A/iPP	100	169.8	156.4	48.63
	50	169.8	155.6	44.25
0.1 %NT-C/iPP	100	169.1	156.6	75.61
	50	169.5	156.0	69.74

below T_R^* (100–105 °C), which leads to significantly smaller and erroneous β -phase content. The shoulder peak at about 175 °C on the curve (NT-C 50 °C) in Fig. 10 indicates the melting of recrystallized α -phase. This proves the conclusion pointed out by Varga et al. [7, 35] that the appearance of the tendency to $\beta\alpha$ -recrystallization of β -PP cooled below T_R^* disturbs the melting profile and prevents the reliable estimation of polymorphic composition.

The isothermal crystallization kinetics of β -iPP samples with mixed polymorphic composition were solved by WAXS technique [47] and isothermal stepwise crystallization method [48], respectively. The evaluation of the crystallization kinetics of α - and β -phases separately according to Avrami method was realized. The non-isothermal crystallization kinetics of β -nucleated PP were reported in the literatures [20, 22, 24, 28, 31]. When the end cooling temperatures in the literatures are below T_R^* , β - α recrystallization occurs. And β and α modifications are formed simultaneously during crystallization. Since the growth rate of the two modifications is different, the polymorphic composition of the sample is changing continuously. It is difficult to separate the non-isothermal crystallization kinetics of α - and β -phases. Therefore, the analysis of the non-isothermal crystallization kinetics of β -iPP samples with mixed polymorphic composition is questionable.

Considering the incomplete crystallization when the cooling rate is $\geq 10\text{ }^\circ\text{C/min}$ for pure iPP and $\geq 15\text{ }^\circ\text{C/min}$ for nucleated iPP samples, the end cooling temperature was chosen as 50 °C in this study. Consequently, considerable errors may be present in the analysis.

Conclusions

In this paper, DSC was used to study the non-isothermal crystallization and subsequent melting behavior of pure iPP and β -nucleated iPP. Non-isothermal crystallization kinetics was analyzed by Jeziorny, Ozawa, and Mo methods, and the activation energy and the nucleating activity were calculated by Kissinger method and Dobрева method, respectively. Following results can be concluded:

- (1) Crystallization temperature decreases and crystallization rate increases with increasing cooling rate, both crystallization temperature and crystallization rate increase with addition of β -nucleating agent;
- (2) Mo method can describe non-crystallization kinetics of pure iPP and nucleated iPP well;
- (3) Addition of NT-A increases ΔE , while NT-C decreases ΔE ;
- (4) Both NT-A and NT-C are effective β -nucleating agents, and NT-C is more effective than NT-A.
- (5) Non-isothermal crystallization kinetics of α - and β -phases cannot be separated, thus the results should be considered with caution.

References

1. Norton DR, Keller A. The spherulitic and lamellar morphology of melt-crystallized isotactic polypropylene. *Polymer*. 1985;26:704–16.
2. Lovinger AJ, Chua JO, Gryte CC. Studies on the α - and β -forms of isotactic polypropylene by crystallization in temperature gradient. *J Polym Sci: Polym Phys Ed*. 1977;15:641–56.
3. Varga J, Karger-Kocsis J. Rules of supermolecular structure formation in sheared isotactic polypropylene melts. *J Polym Sci B*. 1996;34:657–70.
4. Leugering HJ. Einfluss der Kristallstruktur und Überstruktur auf einige Eigenschaften von Polypropylen. *Makromol Chem*. 1967;109:204–16.
5. Fujiyama M. Structures and properties of injection moldings of β -crystal nucleator-added polypropylenes. Part 1. Effect of β -crystal nucleator content. *Int Polym Proc*. 1995;X:172–8.
6. Fujiyama M. Structures and properties of injection moldings of β -crystal nucleator-added polypropylenes. Part 3. Comparison of nucleating effect between γ -quinacridone and quinacridonequinone. *Int Polym Proc*. 1996;XI:271–4.
7. Varga J, Menyhard A. Effect of solubility and nucleating duality of N,N' -dicyclohexyl-2,6-naphthalenedicarboxamide on the supermolecular structure of isotactic polypropylene. *Macromolecules*. 2007;40:2422–31.
8. Lu Q, Dou Q. Crystalline form transformation of isotactic polypropylene induced by N,N' -diphenyl glutaramide. *e-Polymers*. 2008;76:1–11.
9. Dou Q. Effect of N,N' -diphenyl adipamide on the formation of the β -crystalline form in isotactic polypropylene. *J Appl Polym Sci*. 2009;111:1738–44.
10. Lu Q, Dou Q. β -crystal formation of isotactic polypropylene induced by N,N' -dicyclohexylsuccinamide. *J Polym Res*. 2009;16:555–60.
11. Varga J, Stoll K, Menyhard A, Horvath Z. Crystallization of isotactic polypropylene in the presence of β -nucleating agent based on a trisamide of trimesic acid. *J Appl Polym Sci*. 2011;121:1469–80.
12. Shi G, Zhang X, Qiu Z. Crystallization kinetics of β -phase polypropylene. *Makromol Chem*. 1992;193:583–91.
13. Varga J, Mudra I, Ehrenstein GW. Highly active thermally stable β nucleating agents for isotactic polypropylene. *J Appl Polym Sci*. 1999;74:2357–68.
14. Menyhárd A, Varga J, Molnár G. Comparison of different β -nucleators for isotactic polypropylene, characterisation by DSC and temperature-modulated DSC (TMDSC) measurements. *J Therm Anal Calorim*. 2006;83:625–30.
15. Dou Q. Effect of metallic salts of pimelic acid and crystallization temperatures on the formation of β crystalline form in isotactic poly(propylene). *J Macromol Sci B*. 2007;46:1063–80.
16. Dou Q, Lu QL, Li HD. Effect of metallic salts of malonic acid on the formation of β crystalline form in isotactic polypropylene. *J Macromol Sci B*. 2008;47:900–12.
17. Dou Q, Lu QL, Li HD. Effect of metallic salts of glutaric acid on the formation of β -crystalline form in isotactic polypropylene. *J Elastomers Plast*. 2009;41:509–22.
18. Feng JC, Chen MC, Huang ZT, Guo YQ, Hu HQ. Effects of mineral additives on the β -crystalline form of isotactic polypropylene. *J Appl Polym Sci*. 2002;85:1742–8.
19. Zeng AR, Zheng YY, Qiu SC, Guo Y. Isothermal crystallization and melting behavior of polypropylene with lanthanum complex of cyclodextrin derivative as a β -nucleating agent. *J Appl Polym Sci*. 2011;121:3651–61.
20. Zhang Z, Chen CY, Wang CG, Guo JQ, Mai KC. Nonisothermal crystallization kinetics of isotactic polypropylene nucleated with a novel supported β -nucleating agent. *J Therm Anal Calorim*. 2011;103:311–8.
21. Duan QJ, Wang B, Hong BD, Wang HP. Studies on the non-isothermal crystallization behavior of polypropylene/multiwalled carbon nanotubes nanocomposites. *J Macromol Sci B*. 2010;49:1094–104.
22. Xu LL, Zhang XJ, Xu K, Lin SQ, Chen MC. Variation of non-isothermal crystallization behavior of isotactic polypropylene with varying β -nucleating agent content. *Polym Int*. 2010;59:1441–50.
23. Qin J, Chen XL, Yu J, Wang Y, Tian YZ, Wu S. Nonisothermal crystallization kinetics of isotactic polypropylene containing nucleating agent and dispersant. *J Appl Polym Sci*. 2010;117:1047–54.
24. Tjong SC, Xu SA. Non-isothermal crystallization kinetics of calcium carbonate-filled β -crystalline phase polypropylene composites. *Polym Int*. 1997;44:95–103.
25. Ahangari MG, Fereidoon A, Kordani N, Garmabi H. Effect of nano-nucleating agent addition on the isothermal and nonisothermal crystallization kinetics of isotactic polypropylene. *Polym Bull*. 2011;66:239–58.
26. Yang ZG, Zhang ZS, Tao YJ, Mai KC. Effects of polyamide 6 on the crystallization and melting behavior of β -nucleated polypropylene. *Eur Polym J*. 2008;44:3754–63.
27. Yang ZG, Mai KC. Nonisothermal crystallization and melting behavior of β -nucleated isotactic polypropylene and polyamide 66 blends. *J Appl Polym Sci*. 2011;119:3566–73.
28. Yi QF, Wen XJ, Dong JY, Han CC. A novel effective way of comprising β -nucleating agent in isotactic polypropylene (i-PP): polymerized dispersion and polymer characterization. *Polymer*. 2008;49:5053–63.
29. Tao YJ, Pan YX, Zhang ZS, Mai KC. Non-isothermal crystallization, melting behavior and polymorphism of polypropylene in β -nucleated polypropylene/recycled poly(ethylene terephthalate) blends. *Eur Polym J*. 2008;44:1165–74.
30. Yang ZG, Chen CY, Liang DW, Zhang ZS, Mai KC. Melting characteristic and β -crystal content of β -nucleated polypropylene/polyamide 6 alloys prepared using different compounding methods. *Polym Int*. 2009;58:1366–72.
31. Zhao SC, Cai Z, Xin Z. A highly active novel β -nucleating agent for isotactic polypropylene. *Polymer*. 2008;49:2745–54.
32. Shan HF, Lickfield GC. Crystallization kinetics study of polyethylene. *Int J Polym Anal Charact*. 2007;12:327–38.
33. Supaphol P, Thanomkiat P, Phillips RA. Influence of molecular characteristics on non-isothermal melt-crystallization kinetics of syndiotactic polypropylene. *Polym Test*. 2004;23:881–95.

34. Zhang YF, Li X, Wei XS. Non-isothermal crystallization kinetics of isotactic polypropylene nucleated with 1,3:2,4-bis(3,4-dimethylbenzylidene) sorbitol. *J Therm Anal Calorim.* 2010;100:661–5.
35. Varga J. Melting memory effect of the β -modification of polypropylene. *J Therm Anal.* 1986;31:165–72.
36. Avrami M. Kinetics of phase change. I. General theory. *J Chem Phys.* 1939;7:1103–12.
37. Avrami M. Kinetics of phase change. II. Transformation-time relation for random distribution of nuclei. *J Chem Phys.* 1940;8:212–24.
38. Avrami M. Kinetics of phase change. III. Granulation, phase change and microstructure. *J Chem Phys.* 1941;99:177–84.
39. Jeziorny A. Parameters characterizing the kinetics of the non-isothermal crystallization of poly(ethylene terephthalate) determined by DSC. *Polymer.* 1978;19:1142–4.
40. Ozawa T. Kinetics of non-isothermal crystallization. *Polymer.* 1971;12:150–8.
41. Liu TX, Mo ZS, Zhang HF. Nonisothermal crystallization behavior of a novel poly(aryl ether ketone): PEDEKMK. *J Appl Polym Sci.* 1998;67:815–21.
42. Wang JB, Dou Q. Nonisothermal crystallization kinetics and melting behaviors of isotactic polypropylene/ N,N',N'' -tris-tert-butyl-1,3,5-benzene-tricarboxamide. *J Macromol Sci B.* 2008;47:629–42.
43. Kissinger H. Variation of peak temperature with heating rate in differential thermal analysis. *J Res Natl Bur Stand.* 1956;57:217–21.
44. Wei ZY, Zhang WX, Chen GY, Liang JC, Yang S, Wang P, Liu LA. Crystallization and melting behavior of isotactic polypropylene nucleated with individual and compound nucleating agents. *J Therm Anal Calorim.* 2010;102:775–83.
45. Dobrev A, Gutzow I. Activity of substrates in the catalyzed nucleation of glass-forming melts. I. Theory. *J Non-Cryst Solids.* 1993;162:1–12.
46. Dobrev A, Gutzow I. Activity of substrates in the catalyzed nucleation of glass-forming melts. II. Experimental evidence. *J Non-Cryst Solids.* 1993;162:13–25.
47. Chen YH, Mao YM, Li ZM, Hsiao BS. Competitive growth of α and β -crystals in β -nucleated isotactic polypropylene under shear flow. *Macromolecules.* 2010;43:6760–71.
48. Menyhárd A, Dora G, Horváth Z, Faludi G, Varga J. Kinetics of competitive crystallization of β - and α -modifications in β -nucleated iPP studied by isothermal stepwise crystallization technique. *J Therm Anal Calorim.* 2012. doi:10.1007/s10973-011-1900-3.